Liver regeneration during the associating liver partition and portal vein ligation for staged hepatectomy procedure in *Sus scrofa* is positively modulated by stem cells

MARTIN BARTAS[1], JIRI ČERVEŇ[1,2], JAN OPPELT[3,4], MATUS PETEJA[5,6], PETR VÁVRA[5,6], PAVEL ZONČA[5,6], VACLAV PROCHÁZKA[7], VACLAV BRÁZDA[8] and PETR PEČINKA[1,2]

[1]Department of Biology and Ecology; [2]Institute of Environmental Technologies, Faculty of Science, University of Ostrava, 71000 Ostrava; [3]Centre for Structural Biology, Central European Institute of Technology; [4]National Centre for Biomolecular Research, Centre for Structural Biology, Central European Institute of Technology, Masaryk University, 62500 Brno; [5]Department of Surgery, University Hospital in Ostrava; [6]Department of Surgical Studies, Faculty of Medicine, University of Ostrava; [7]Department of Radiology, University Hospital in Ostrava, 70852 Ostrava; [8]Institute of Biophysics, Academy of Sciences of The Czech Republic, 61265 Brno, Czech Republic

Abstract. This present study investigated the impact of the application of stem cells to liver regeneration following the first stage of associating liver partition and portal vein ligation for staged hepatectomy (ALPPS). The experiment was conducted on a pig model (n=6, 3 that did not receive application of stem cells, 3 that received application stem cells). Collected samples of liver (day 0 and 9 following surgery) were subjected to complete transcriptome sequencing. In total, 39 differentially expressed genes were found in the group without the application of the stem cells (genes of unwanted processes such as fibrosis and inflammation). In the group that did receive application of stem cells, no significantly differentially expressed genes were found, indicating a properly regenerated liver remnant. The present study therefore demonstrated, to the best of our knowledge for the first time, the positive effect of stem cells application in the liver regeneration process during ALPPS procedure in the pig model.

Correspondence to: Professor Petr Pečinka, Department of Biology and Ecology, Faculty of Science, University of Ostrava, 10 Chittussiho Street, 71000 Ostrava, Czech Republic
E-mail: petr.pecinka@osu.cz

Introduction

The process of liver regeneration is, on the molecular level, an extremely complicated process that requires a perfect interplay of cell-cell signaling and gene expression continuity (1). Liver regeneration has traditionally been divided into three phases: Initiation, proliferation and termination (2). The duration of these phases depends on the organism under examination, including human, pig or rat, and the type of surgical intervention, including partial hepatectomy, intoxication by drugs, or hereditary predispositions (3). The organisms most frequently used to investigate liver regeneration are rats and mice, which are relatively well-investigated model organisms. However, pigs (*Sus scrofa*) are anatomically and physiologically closer to humans than rodents, and therefore are attractive subjects for biomedical research, despite the higher cost of maintenance (4). Budai *et al* (5) outlines a detailed comparison of existing associating liver partition and portal vein ligation for staged hepatectomy (ALPPS) animal models and their advantages.

Currently, it is known that application of adipose-derived stem cells may positively modulate tissue regeneration processes (6-8). There are a number of clinical studies that are aimed at verifying the safety and effectiveness of this form of treatment; however, the molecular mechanisms of action remain largely unclear (9,10). It is likely to be the primarily paracrine mechanism of action that produces growth factors and cytokines, which positively modulate regenerative processes, such as improved angiogenesis, and limit inflammatory processes (9,10).

The present study analyzed the effect of the application of stromal vascular fat tissue stem cells on liver regeneration during the first stage of ALPPS procedure. ALPPS is a relatively recent modification of the two-staged hepatectomy, first described in 2010 (11). ALPPS approach allows for surgery on severe liver tumor burden in two associated steps. In the first step, tumor loci are removed

from less affected liver lobe, the two liver lobes are split by parenchyma transection and the more metastatic region of the liver is deportalized. Deportalization of one liver lobe stimulates the second liver lobe to undergo hypertrophic regeneration (the future liver remnant). The patient is then permitted 1 or 2 weeks to recover. The second step removes the deportalized region of the liver, while the hypertrophic future liver remnant is fully functional (12). This approach significantly increases possibility of curative treatment of severe liver tumor diseases (13).

It is assumed that the application of stem cells obtained from stromal vascular fat tissue accelerates the regenerative process by allowing for improved angiogenesis and modulation of inflammation, as has been previously observed in animal-model studies (14,15); however, to the best of our knowledge, this has not been demonstrated in direct connection with ALPPS approach and *Sus scrofa* model organism. The aim of the present study was to identify candidate genes that may be used as screening markers for monitoring the process of liver regeneration following the first stage of ALPPS.

Materials and methods

Animals. A total of six juvenile domestic swine (Polish white pigs; 6 months; seven females and one castrated male; weight 30-50 kg; Instytut Zootechniki, Grodziec Śląski, Poland) were included in the present study. The pigs were housed in separated boxes at room temperature (15-20˚C), air humidity of 50-60%, normal atmosphere, 12 h light/dark cycles and access to food and water *ad libidum*. Procedures were performed in the Center for Cardiovascular Research and Development, American Heart of Poland S.A. (Ustroń, Poland) between September and October 2014. Approval from the Bioethical Committee from the Center for Cardiovascular Research and Development, American Heart of Poland S.A. (Ustroń, Poland) was obtained. Animals were assigned to two groups: n=3 without stem cell application (pig nos. 1-3) and n=3 with stem cell application (pig nos. 4-6), based on their identification numbers. All animals received an acclimation period of 3 days prior to any procedures, during which and no premedication was administered. Animals were anesthetized following an overnight fast (water was not withheld) based on their body weight using ketamine (20 mg/kg), xylazine (2 mg/kg) and atropine (1 mg/pig). Propofol was also administered as a bolus (1 mg/kg) prior to intubation to induce muscle relaxation. General anesthesia was maintained during procedures with a constant infusion drip of propofol. Fentanyl (100 µg/pig) was administered at the beginning of each procedure to potentiate anesthesia and as an analgesic, and all animals received mechanical ventilation support throughout the procedures. At pre-determined time-points the animals were euthanized with pentobarbital solution (140 mg/kg), and livers were harvested for histological and whole transcriptome analysis. Pigs were necropsied and examined for abnormal findings, and were labeled with the animal identification number, protocol number and date of collection.

ALPPS first phase. Pigs were anaesthetized as aforementioned. Laparotomy and investigation of the abdominal organs was

performed, and revision of the liver was conducted, with the preparation of the liver hilus, identification of the portal vein and its branching, identification of the bile duct and hepatic arteries. Confirmation of the injection site was performed by venography using contrast medium (iopromidum) and C-arm fluoroscopy. The entry of hepatic veins into vena cava inferior was identified. The flow of portal blood into four lobes of the liver was interrupted; only the inflow of portal blood into the one selected hepatic lobe (future liver remnant) was preserved. This procedure was followed by splitting of liver between the lobe with preserved perfusion through the portal vein and other lobes, to which the inflow of portal blood was closed. Samples of liver tissue were harvested from the future liver remnant lobes and were stored snap-frozen using liquid nitrogen (-196˚C) in a tissue bank. Furthermore, 15 ml of the human adipose stem cells-stromal vascular fraction concentrate (Cytori Therapeutics, Inc., San Diego, CA, USA) was administered intra-arterially to the group of animals with planned administration of stem cells via the hepatic artery during the surgery procedure. For more information about characteristics of this concentrate see a previous study by Lin *et al* (16). The animals in the group that did not undergo stem cell application were administered 15 ml of saline via an identical route of administration. Hydrocortisone was applied intravenously prior to the administration of stem cells to prevent an autoimmune reaction (rejection). The animals were monitored postoperatively by measuring body temperature (*per rectum*) and weight daily.

ALPPS second phase. Surgery was performed 9 days after the first stage. Re-laparotomy and investigation of abdominal organs were performed, together with liver revision and identification of pre-marked structures in the hilus and entry of hepatic veins into the vena cava inferior. In total, four liver lobes were removed with the perfused lobe remaining in place.

Tissue sampling, RNA isolation and whole transcriptome sequencing. All samples of liver tissue were collected into separate 5 ml polypropylene tubes prefilled with equivalent volume of RNA later solution and stored at -20˚C. Isolation of total RNA was performed using the QuickGene Mini 80 semi-automatic device and appropriate RNA tissue kit SII (both from Kurabo Industries Ltd., Osaka, Japan). RNA concentration and integrity were determined using the Agilent 2100 Bioanalyzer (Agilent Technologies, Inc., Santa Clara, CA, USA). RNA-sequencing libraries preparation and cDNA sequencing was performed by Macrogen, Inc. (Seoul, Republic of Korea), resulting in a set of 101 nucleotide paired-end-read data files.

Transcriptome data analysis. The quality of the raw sequencing data was assessed using FastQC (v0.11.5) (17) and aligned to a reference genome of *Sus scrofa* (Ensembl v82; *Sus scrofa* 10.2) using the STAR aligner (v2.4.1b) (18). Up to five mapping reads were used for subsequent analyses. Raw gene counts were obtained by calculating reads mapping to exons and summarized by genes using reference gene annotation (Ensembl v.82, *Sus scrofa* assembly, GTF) by featureCounts (v1.4.6-p5) (19). Differential gene expression was
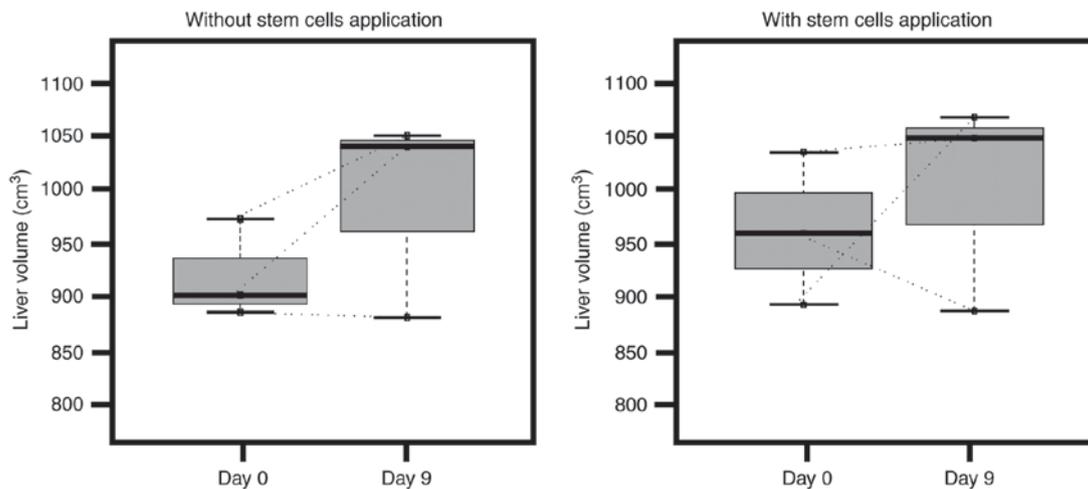
Figure 1. Total liver volume measurement by magnetic resonance imaging in the group that did not receive stem cell application (left side; paired Wilcoxon test, P=0.23) and the group that did (right side; paired Wilcoxon test, P=0.65). Dashed lines illustrate sample pairing. Measurements were made prior to the first stage (day 0) and prior to the second stage (day 9) of ALPPS. In the two cases, paired t-test P-values were not significant, which was likely due to low number of biological replicates.

calculated using edgeR (v3.10.5) (20). Two states (day 0 and 9) within each experimental group of animals were compared. False discovery rate (FDR) correction was used to correct the P-values for multiple assessments. Genes were determined as differentially expressed when the FDR adjusted P-value ≤0.1 and $\log_2$ fold-change ($\log_2$FC) ≥0.5. Pathway analyses were performed in STRING (v10.5) (21,22), Panther (23) with the aid of Kyoto Encyclopedia of Genes and Genomes (KEGG) (24,25).

Volumetric measurements. All magnetic resonance imaging (MRI) experiments were performed using a 1.5 T scanner (GE Healthcare, Chicago, IL, USA), and an eight-channel phased array head coil was used. MRI measurements were performed at baseline (day 0) and on day 9, prior to second ALPPS stage.

Statistical analysis. The non-parametric paired Wilcoxon test was used for statistical comparison of changes in liver volume between day 0 and 9. According to the experimental design, this comparison was performed separately for the group that did not receive the application of stem cells and for the group that did. Software R was used for statistical analysis (version 3.4.1; The R Foundation for Statistical Computing, Wien, Austria). P<0.05 was considered to indicate a statistically significant difference. Data in the barplots are presented as the mean ± standard deviation.

Results

Although each step of the ALPPS procedure was performed successfully, no significant changes in total liver volume were observed following the first ALPPS stage (Fig. 1) (P=0.5 without application of stem cells; P=0.75 with application of stem cells). This may be due to the fact that only future liver remnants are expected to increase in size over a longer period of time.

Comprehensive transcriptome analysis of samples from future liver remnant was performed to examine for changes in the gene expression between groups with and without application of stem cells. We hypothesized that the application of stem cells would accelerate liver regeneration by inhibition of undesirable processes, such as fibrosis and inflammation.

A total of 39 significantly differentially expressed genes were identified in the group without application of stem cells between day 0 and 9 (Table I), there of 37 genes were upregulated and two downregulated. In the group with stem cell treatment there were no differentially expressed genes between day 0 and 9. The highest significantly different gene expression was observed for collagen type IV α1 chain (COL4A1). COL4A1, COL4A2, laminin subunit γ1 and nidogen 2 (all of which were upregulated; Fig. 2) form major components of the basement membrane (with COL4A1 and COL4A2 constituting a functional heterotrimer with 2:1 stoichiometry) (26,27). The greatest positive change (upregulation) in the gene expression was for latent transforming growth factor-β binding protein 2 (LTBP2) and the greatest negative change (downregulation) was for heme binding protein 2. LTBP2 together with thrombospondin 1, transglutaminase 2 and fibrillin 1, all of which were upregulated (detailed changes in gene expression are depicted in Fig. 3) and serve an important role in the transforming growth factor-β pathway in the extracellular matrix remodeling process (28).

Functional classification revealed that the majority of differentially expressed genes from the group of pigs that received the application of stem cells are associated with their functional interactions and localization (primarily in the extracellular matrix and cytoplasmic membrane); Fig. 4 contains a detailed interactome, with mainly collagens making up a strong interaction network. Analysis of molecular functions revealed 19 significantly enrichment categories, as 'growth factor binding', 'extracellular matrix structural constituent' or 'semaphorin receptor activity' (Table II). This is in congruence with a previous study by Rychtrmoc *et al* (29), where they observed changes in expression in a number of genes

Table I. Significantly differentially expressed genes in the group without application of stem cells between day 0 and 9, sorted by lowest FDR value.

Identifier	Symbol	Gene name	$\log_2$ FC	FDR
ENSSSCG00000009544	COL4A1	Collagen, type IV, α1	0.93	0.00
ENSSSCG00000007000	FAT1	FAT tumor suppressor homolog 1 (*Drosophila*)	0.78	0.01
ENSSSCG00000000712	VWF	Von Willebrand factor	1.15	0.01
ENSSSCG00000023522	TGM2	Transglutaminase 2	0.75	0.01
ENSSSCG00000004658	FBN1	Fibrillin 1	0.94	0.01
ENSSSCG00000011859	HEG1	HEG homolog 1 (zebrafish)	0.95	0.01
ENSSSCG00000001725	GPR116	G protein-coupled receptor 116	0.69	0.01
ENSSSCG00000009545	COL4A2	Collagen, type IV, α2	0.84	0.01
ENSSSCG00000014442	PDGFRB	Platelet-derived growth factor receptor, β-polypeptide	0.82	0.01
ENSSSCG00000028022	COL6A2	Collagen, type VI, α2	0.74	0.02
ENSSSCG00000002368	LTBP2	Latent transforming growth factor-β binding protein 2	1.64	0.02
ENSSSCG00000004150	HEBP2	Heme binding protein 2	-1.09	0.02
ENSSSCG00000008749	SLIT2	Slit homolog 2 (*Drosophila*)	1.28	0.02
ENSSSCG00000011443	STAB1	Stabilin 1	0.84	0.02
ENSSSCG00000005751	COL5A1	Collagen, type V, α1	0.76	0.03
ENSSSCG00000009045	HHIP	Hedgehog interacting protein	0.71	0.03
ENSSSCG00000004387	FOXO3A	Forkhead box O3	0.65	0.04
ENSSSCG00000001834	MFGE8	Milk fat globule-EGF factor 8 protein	0.74	0.04
ENSSSCG00000027969	AHNAK	AHNAK nucleoprotein	0.91	0.04
ENSSSCG00000009320	FLT1	Fms-related tyrosine kinase 1	0.85	0.04
ENSSSCG00000004091	AKAP12	A kinase (PRKA) anchor protein 12	0.81	0.04
ENSSSCG00000028239	FBXL7	F-box and leucine-rich repeat protein 7	1.10	0.04
ENSSSCG00000011075	KIAA1217	Kiaa1217	0.61	0.04
ENSSSCG00000022000	COL1A2	Collagen, type I, α2	0.80	0.05
ENSSSCG00000029189	DCHS1	Dachsous 1 (*Drosophila*)	0.91	0.05
ENSSSCG00000017548	NGFR	Nerve growth factor receptor	0.79	0.05
ENSSSCG00000009111	SYNPO2	Synaptopodin 2	0.91	0.06
ENSSSCG00000015068	APOA4	Apolipoprotein A-IV	-0.62	0.06
ENSSSCG00000015555	LAMC1	Laminin, γ1	0.74	0.07
ENSSSCG00000005030	NID2	Nidogen 2 (osteonidogen)	0.68	0.07
ENSSSCG00000011102	NRP1	Neuropilin 1	0.55	0.08
ENSSSCG00000026383	NRP2	Neuropilin 2	0.78	0.08
ENSSSCG00000015326	COL1A2	Collagen, type I, α2	0.78	0.09
ENSSSCG00000027331	COL6A3	Collagen, type VI, α3	0.71	0.09
ENSSSCG00000011743	MECOM	MDS1 and EVI1 complex locus	1.28	0.09
ENSSSCG00000005494	TNC	Tenascin C	1.40	0.10
ENSSSCG00000015426	RELN	Reelin	0.61	0.10
ENSSSCG00000016035	COL5A2	Collagen, type V, α2	0.67	0.10
ENSSSCG00000004789	THBS1	Thrombospondin 1	1.10	0.10

$\log_2$FC >|0.5| and FDR <0.1 were chosen as a threshold. $\log_2$FC, $\log_2$ fold change; FDR, false discovery rate.

involved in extracellular matrix remodeling pathways in liver regeneration termination using microarray and reverse transcription-quantitative polymerase chain reaction analysis in a rat model (29). At the level of biological processes the most relevant significantly enriched categories were 'anatomical structure morphogenesis', 'circulatory system development' and 'axon development' (Table III). The most enriched KEGG pathways were 'PI3K-Akt signaling pathway',

Table II. Molecular function enrichment in the group without application of stem cells between day 0 and 9, sorted by FDR value.

Pathway ID	Pathway description	Observed gene count	FDR	Matching proteins
GO.0019838	Growth factor binding	8	5.25×10^{-9}	COL1A2, COL4A1, COL5A1, FLT1, NRP1, NRP2, DGFRB, THBS1
GO.0048407	Platelet-derived growth factor binding	4	4.28×10^{-6}	COL1A2, COL4A1, COL5A1, PDGFRB
GO.0005539	Glycosaminoglycan binding	7	3.18×10^{-5}	COL5A1, LTBP2, NRP1, NRP2, SLIT2, STAB1, THBS1
GO.0005201	Extracellular matrix structural constituent	5	6.82×10^{-5}	COL1A2, COL4A1, COL4A2, COL5A1, FBN1
GO.0097493	Structural molecule activity conferring elasticity	3	6.88×10^{-5}	AHNAK, COL4A1, FBN1
GO.0005021	Vascular endothelial growth factor-activated receptor activity	3	8.59×10^{-5}	FLT1, NRP1, NRP2
GO.0008201	Heparin binding	6	8.59×10^{-5}	COL5A1, LTBP2, NRP1, NRP2, SLIT2, THBS1
GO.0005515	Protein binding	21	0.000139	AHNAK, AKAP12, APOA4, COL1A2, COL4A1, COL5A1, FBN1, FLT1, FOXO3, HHIP, MECOM, NGFR, NID2, NRP1, NRP2, PDGFRB, RELN, SLIT2, SYNPO2, THBS1, TNC
GO.0005509	Calcium ion binding	9	0.00039	DCHS1, FAT1, FBN1, HEG1, LTBP2, MECOM, NID2, SLIT2, THBS1
GO.0043394	Proteoglycan binding	3	0.000866	COL5A1, SLIT2, THBS1
GO.0004714	Transmembrane receptor protein tyrosine kinase activity	4	0.00106	FLT1, NRP1, NRP2, PDGFRB
GO.0030023	Extracellular matrix constituent conferring elasticity	2	0.0044	COL4A1, FBN1
GO.0038085	Vascular endothelial growth factor binding	2	0.0044	NRP1, PDGFRB
GO.0046872	Metal ion binding	17	0.0117	APOA4, COL1A2, COL5A1, DCHS1, FAT1, FBN1, HEG1, HHIP, LTBP2, MECOM, NID2, NRP1, NRP2, RELN, SLIT2, TGM2, THBS1
GO.0017154	Semaphorin receptor activity	2	0.0259	NRP1, NRP2
GO.0019955	Cytokine binding	3	0.0335	NRP1, NRP2, THBS1
GO.0005178	Integrin binding	3	0.0461	COL5A1, FBN1, THBS1
GO.0005198	Structural molecule activity	6	0.0461	AHNAK, COL1A2, COL4A1, COL4A2, COL5A1, FBN1
GO.0030169	Low-density lipoprotein particle binding	2	0.0476	STAB1, THBS1

FDR=0.05 was chosen as a threshold. FDR, false discovery rate.

Table III. Biological process enrichment in the group without application of stem cells between day 0 and 9, sorted by lowest FDR value.

Pathway ID	Pathway description	Observed gene count	FDR	Matching proteins
GO:0009653	Anatomical structure morphogenesis	21	7.36×10^{-10}	COL1A2, COL4A1, COL4A2, COL6A2, COL6A3, DCHS1, FAT1, FBN1, FLT1, FOXO3, HEG1, HHIP, MECOM, NGFR, NRP1, NRP2, PDGFRB, SLIT2, TGM2, THBS1, TNC
GO:0072358	Cardiovascular system development	14	1.8×10^{-8}	COL1A2, COL4A1, COL4A2, COL5A1, DCHS1, FBN1, FLT1, HEG1, MECOM, NRP1, NRP2, PDGFRB, SLIT2, THBS1
GO:0072359	Circulatory system development	14	1.8×10^{-8}	COL1A2, COL4A1, COL4A2, COL5A1, DCHS1, FBN1, FLT1, HEG1, MECOM, NRP1, NRP2, PDGFRB, SLIT2, THBS1
GO:0044243	Multicellular organismal catabolic process	7	1.38×10^{-7}	APOA4, COL1A2, COL4A1, COL4A2, COL5A1, COL6A2, COL6A3
GO:0001568	Blood vessel development	11	1.51×10^{-7}	COL1A2, COL4A1, COL4A2, COL5A1, FLT1, HEG1, NRP1, NRP2, PDGFRB, SLIT2, THBS1
GO:0001944	Vasculature development	11	1.58×10^{-7}	COL1A2, COL4A1, COL4A2, COL5A1, FLT1, HEG1, NRP1, NRP2, PDGFRB, SLIT2, THBS1
GO:0006935	Chemotaxis	12	1.58×10^{-7}	COL4A1, COL4A2, COL5A1, COL6A2, COL6A3, FLT1, NGFR, NRP1, NRP2, PDGFRB, RELN, SLIT2
GO:0030198	Extracellular matrix organization	10	1.72×10^{-7}	COL1A2, COL4A1, COL4A2, COL5A1, COL6A2, COL6A3, FBN1, NID2, THBS1, TNC
GO:0061564	Axon development	11	2.00×10^{-7}	COL4A1, COL4A2, COL5A1, COL6A2, COL6A3, NGFR, NRP1, NRP2, RELN, SLIT2, TNC
GO:0007411	Axon guidance	10	3.15×10^{-7}	COL4A1, COL4A2, COL5A1, COL6A2, COL6A3, NGFR, NRP1, NRP2, RELN, SLIT2
GO:0022617	Extracellular matrix disassembly	7	5.34×10^{-7}	COL1A2, COL4A1, COL4A2, COL5A1, COL6A2, COL6A3, FBN1
GO:0040011	Locomotion	14	6.1×10^{-7}	COL1A2, COL4A1, COL4A2, COL5A1, COL6A2, COL6A3, FAT1, FLT1, NGFR, NRP1, NRP2, PDGFRB, SLIT2, THBS1
GO:0048666	Neuron development	12	1.04×10^{-6}	APOA4, COL4A1, COL4A2, COL5A1, COL6A2, COL6A3, MECOM, NGFR, NRP1, NRP2, SLIT2, TNC
GO:0030574	Collagen catabolic process	6	1.23×10^{-6}	COL1A2, COL4A1, COL4A2, COL5A1, COL6A2, COL6A3
GO:0071363	Cellular response to growth factor stimulus	11	1.3×10^{-6}	COL1A2, COL4A2, FBN1, FLT1, FOXO3, LTBP2, MECOM, NGFR, NRP1, NRP2, PDGFRB
GO:0000904	Cell morphogenesis involved in differentiation	11	1.57×10^{-6}	COL4A1, COL4A2, COL5A1, COL6A2, COL6A3, HEG1, NGFR, NRP1, NRP2, RELN, SLIT2
GO:0007409	Axonogenesis	10	1.57×10^{-6}	COL4A1, COL4A2, COL5A1, COL6A2, COL6A3, NGFR, NRP1, NRP2, RELN, SLIT2
GO:0031175	Neuron projection development	11	1.57×10^{-6}	APOA4, COL4A1, COL4A2, COL5A1, COL6A2, COL6A3, NGFR, NRP1, NRP2, SLIT2, TNC
GO:0006928	Movement of cell or subcellular component	14	1.58×10^{-6}	COL1A2, COL4A1, COL4A2, COL5A1, COL6A2, COL6A3, FAT1, FLT1, NGFR, NRP1, NRP2, PDGFRB, SLIT2, THBS1
GO:0048468	Cell development	15	1.79×10^{-6}	APOA4, COL4A1, COL4A2, COL5A1, COL6A2, COL6A3, FOXO3, HEG1, MECOM, NGFR, NRP1, NRP2, PDGFRB, SLIT2, TNC

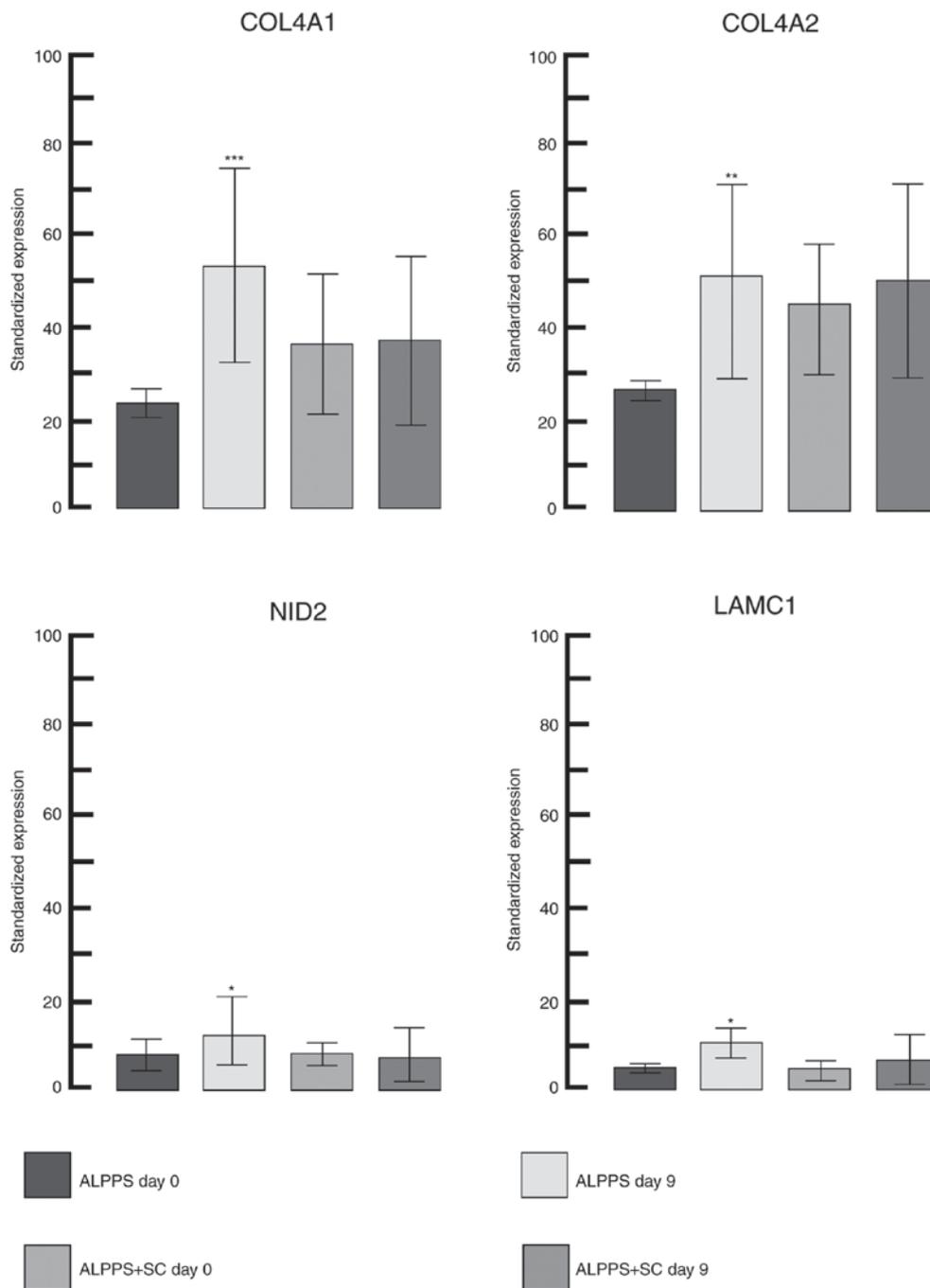The 20 best hits are shown. FDR, false discovery rate.

Figure 2. Significantly differentially expressed genes of the 'basement membrane cluster' in the all groups between day 0 and day 9, within groups only. The plot shows the mean values and standard deviations (*P<0.05, **P<0.01 and ***P<0.001 vs. corresponding control - day 0).

'Focal adhesion' and 'ECM-receptor interaction' (Table IV). The phosphoinositide 3-kinase (PI3K)-RAC serine/threonine-protein kinase (Akt) signaling pathway is likely to drive forward liver regeneration via hepatocyte growth factor stimulation, as observed on rat oval cells *in vitro* (30). Inhibition of the PI3K-Akt pathway disturbed liver regeneration in mice (31).

A more detailed examination of gene expression in specific pigs between day 0 and 9 revealed certain notable facts (only values with a $\log_2$ FC ± 3 with >4 normalized edgeR counts were taken into account). Only certain genes in pig nos. 4 and 6 (that received stem cell treatment) met these more stringent

criteria (Table V). In pig no. 6, there was an extremely large increase in the expression of the RNA component of RNase P and 7S kinase (7SK) RNA. According to Reiner *et al* (32), RNase P may serve an important role in transcription of a number of non-coding RNAs that are transcribed by RNA polymerase III. 7SK RNA is one of the genes transcribed by RNA polymerase III. It is therefore likely that in pig no. 6 there was co-expression of these two genes, which are localized on the same chromosome (RNase P RNA component, chromosome 7:83, 579, 873-83, 580, 200 forward strand; 7SK RNA, chromosome 7:134, 400, 749-134, 401, 079 forward strand). There were also three overexpressed genes for Metazoan
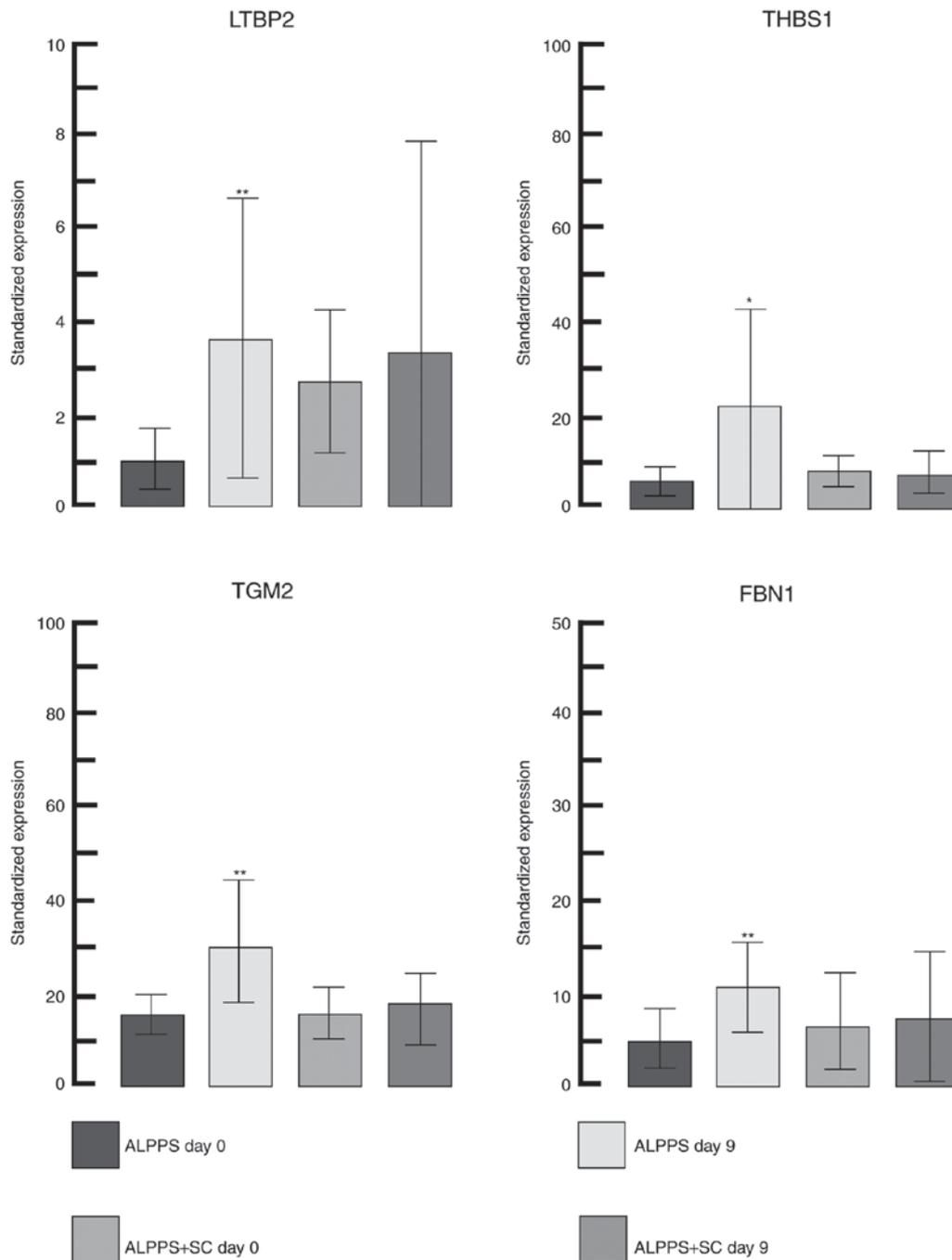
Figure 3. Significantly differentially expressed genes of the 'TGF-β affecting cluster' in the all groups between day 0 and 9, within groups only. The plot shows the mean values and standard deviations (*P<0.05 and **P<0.01).

signal recognition particle RNA (also transcribed by RNA polymerase III). Interleukin-13 receptor subunit α2 was also downregulated in pig no. 6. However, these results for individual pigs cannot conclusively inform on the mode of action of the applied stem cells, but serve as a source of hypotheses for subsequent studies.

Discussion

Although the liver has the ability to regenerate itself, the application of stem cells speeds up the process; this has been demonstrated in the present study via the presence of fewer differentially expressed genes in the presence of stem cells, indicating that the regeneration process is finished or is in the late phase. Timing is crucial in the ALPPS procedure, so faster liver regeneration between stages is highly beneficial. According to the experimental design, no significant changes to liver morphology were expected; as 9 days is too short a period to observe liver fibrosis (33-37), gene expression analyses were performed, which reliably identify expression changes in collagen and other fibrogenic factors before they become visible via microscopy. Previous animal studies demonstrated that microscopic changes to liver structure following intervention were not observed for several weeks (33-37).
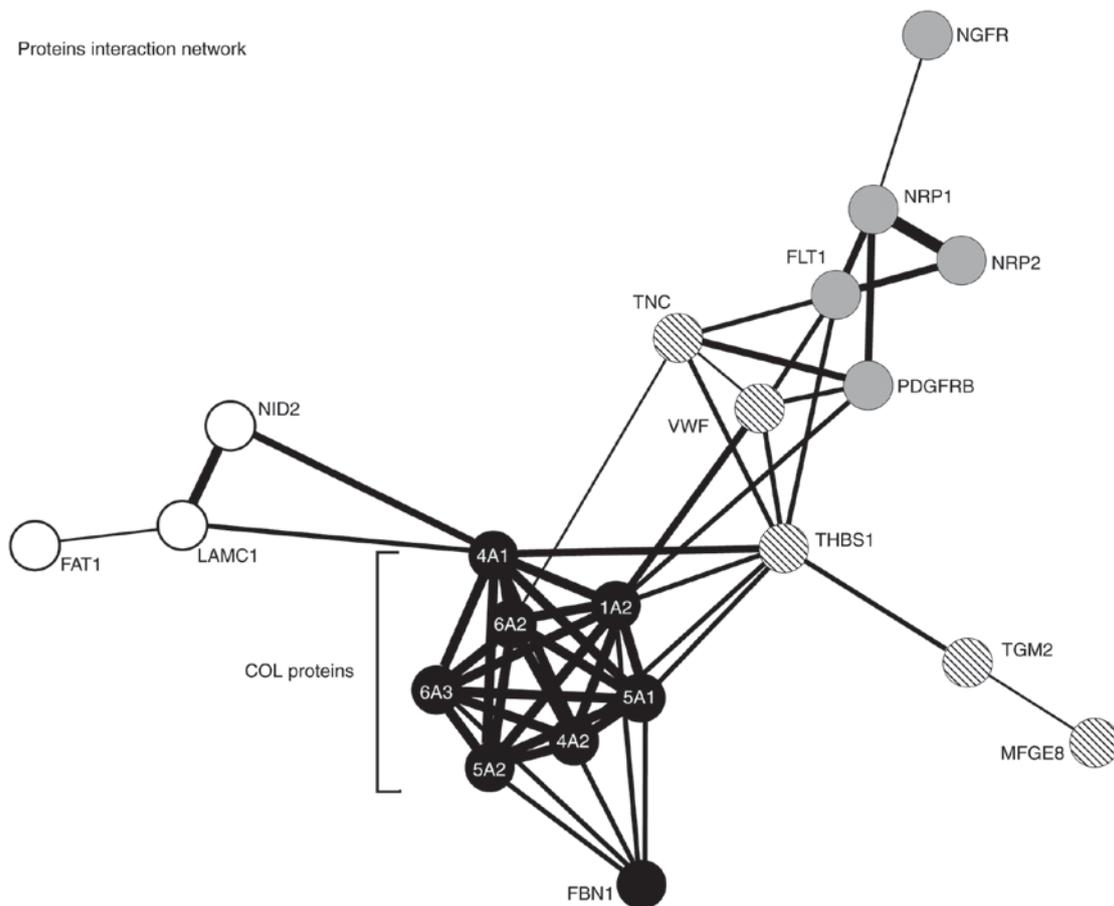
Figure 4. Protein-protein interaction network of 39 significantly differentially expressed genes in the group without application of stem cells (between day 0 and 9). Individual clusters represent structurally or functionally similar proteins (black circles stands for 'collagen' cluster, gray for 'neural and vascular development' cluster, striped for 'TGF-β affecting' cluster and white for 'Other basement membrane proteins' cluster. Thickness of connecting lines depends on the degree of scientific evident for particular connection. Figure was constructed in STRING online v.10.5 (21,22). Disconnected nodes are hidden. Four clusters were made using built in 'k means clustering' function.

Differentially expressed genes in the group of pigs that did not receive stem cell application (between day 0 and 9) encode proteins primarily involved in extracellular matrix remodeling, angiogenic and neurogenic processes. Owing to the fact that in the group that underwent the application of stem cells, there were no differentially expressed genes between day 0 and 9, the application of stem cells seemingly positively modulated the regenerative processes by accelerating regeneration, and preventing an unwanted fibrosis and inflammation processes. To provide more precise interpretation a larger number of biological replicates and more time-points are required (ideally on day 0, 3, 5, 7, 9, 11 and 20 to observe upward/downward trends in gene expression in broader time scale), although in a large animal model, such an approach is limited by financial costs.

Angiogenesis is a process that accompanies liver regeneration process and serves an important role in restoration of vascular networks in the place of liver damage. This process is driven by several pro-angiogenic growth factors. A number of the primary pro-angiogenic factors are vascular endothelial growth factors that bind to their membrane receptors, including Fms-related tyrosine kinase-1 (Flt-1), fetal liver kinase-1 or Flt-4. The present study observed the increased expression of Flt-1 receptor in the group without application

of stem cells between day 0 and 9, which is in congruence of former study in a rat model, in which expression of Flt-1 was significantly increased between day 4 and 10 following 70% hepatectomy (38).

The process of axon guidance in liver regeneration may be mediated by secreted third class semaphorins (Sema3A-G), which bind to a membrane receptor complex whose main component is a transmembrane glycoprotein neuropillin 1 or neuropillin 2, or a heterodimer of the two (39). The interaction between the semaphorins 3A and neuropillin 1 is also notable in the angiogenic processes (40). The present study revealed increased expression of neuropillin 1 and neuropillin 2 in the group without application of stem cells between day 0 and 9.

The remodeling of extracellular matrix serves an important role in the process of liver regeneration. In the initiation stage of liver regeneration, the extracellular matrix is broken down to allow for the proliferation of hepatocytes. Subsequently, the extracellular matrix requires rebuilding to ensure physical support is provided to endothelial cells. Production of extracellular matrix is primarily provided by the population of stellar liver cells. Restoration of the extracellular matrix is manifested by an increased synthesis of collagen, structural glycoproteins and proteoglycans, which occurs mainly between day 3 and 5 following partial hepatectomy in a rat

Table IV. Kyoto Encyclopedia of Genes and Genomes pathway enrichment in the group without application of stem cells between day 0 and 9, sorted by lowest FDR value.

Pathway ID	Pathway description	Observed gene count	FDR	Matching proteins
4151	PI3K–Akt signaling pathway	13	9.81×10^{-13}	COL1A2, COL4A1, COL4A2, COL5A1, COL6A2, COL6A3, FLT1, FOXO3, NGFR, PDGFRB, RELN, HBS1, TNC
4510	Focal adhesion	11	1.49×10^{-12}	COL1A2, COL4A1, COL4A2, COL5A1, COL6A2, COL6A3, FLT1, PDGFRB, RELN, THBS1, TNC
4512	ECM-receptor interaction	9	1.49×10^{-12}	COL1A2, COL4A1, COL4A2, COL5A1, COL6A2, COL6A3, RELN, THBS1, TNC
4974	Protein digestion and absorption	6	3.52×10^{-7}	COL1A2, COL4A1, COL4A2, COL5A1, COL6A2, COL6A3
5146	Amoebiasis	4	0.00149	COL1A2, COL4A1, COL4A2, COL5A1
5200	Pathways in cancer	5	0.00832	COL4A1, COL4A2, HHIP, MECOM, PDGFRB
4015	Rap1 signaling pathway	4	0.0144	FLT1, NGFR, PDGFRB, THBS1

FDR=0.05 was chosen as a threshold. FDR, false discovery rate.

model (41). The present study observed an elevated expression of a number of genes associated with extracellular matrix remodeling between day 0 and day 9 day in the group without application of stem cells.

The application of stem cells in pig no. 6 (that received the application of stem cells) likely decreased the expression of interleukin 13 receptor subunit α2 (IL13RA2). Functional IL13RA2 was overexpressed in activated hepatic stellate cells in rat livers (42). Activated hepatic stellate cells are associated with unwanted liver fibrosis (43). The anti-fibrotic effect of xenogeneic adipose mesenchymal stem cells was recently observed by Maria *et al* (44), whereby a mouse model of systemic sclerosis was used. It would be necessary to use more biological replicates than in the present study to determine more accurately the number of pigs in which this effect occurred. In pig no. 6, rapid co-expression of RNAseP and 7SK functional RNAs (>16 times higher expression) was observed. It would be interesting to examine this observation in similar experiments in the future. However, owing to the limited number of biological replicates, clear interpretation cannot be performed. It is possible, that RNAseP may serve as a major inductor of 7SK RNA expression, as, according to Reiner *et al* (32), RNAseP activates the transcription of RNA polymerase III.

The change in gene expression in pig no. 4 that underwent application of stem cells likely demonstrates the termination of proliferative processes, characterized by the downregulation of Mdm4 p53 binding protein homolog (mouse) and LATS large tumor suppressor homolog 1 (*Drosophila*) and thereby stabilization of the p53 suppressor protein. This also reflects the decreased expression of other transcription factors, including one cut homeobox 1 (ONECUT1) or heart development protein with EGF like domains 1. The overexpression of ONECUT1 was observed in early stages of liver regeneration in a rat model (45). SH3 and PX domains 2A is apparently involved in the production of free radicals as a member of the NADPH oxidase complex complex (46). This finding indicates that the proliferative processes in pig no. 4 were accelerated owing to the application of stem cells and similarly, the formation of undesirable free radicals was limited.

RNA sequencing studies aided the evaluation of gene expression in animal models of variety human clinical conditions, including in the study by Arvaniti *et al* (47), which revealed numerous previously unknown genes associated with renal fibrosis using a mouse model (47). Although the present study encountered limitations including the mortality of one pig due to source contamination and also the corruption of one sequenation data file. These limitations resulted in decreased animal numbers; however, the results obtained may provide insight and could be validated by future studies that build on these findings. Certain differentially expressed genes identified in the present study may serve as molecular markers for monitoring the progress of liver regeneration generally, not only during ALPPS, in human patients. Analysis of differentially expressed genes indicates that the application of stem cells elicited a positive effect in the acceleration of regenerative processes; however, there is a requirement for further experiments to be conducted with more biological replicates and tissue sampling time-points.

Table V. Differentially expressed genes in pig nos. 4 and 6 (that received stem cell treatment) between the day 0 and 9, sorted by highest Log$_2$FC value.

Identifier	Symbol	Gene name	log$_2$FC
ENSSSSCG00000019556	7SK	7SK RNA	4.11
ENSSSSCG00000020439	RNaseP_nuc	Nuclear RNase P	4.02
ENSSSSCG00000024699	Metazoa_SRP	Metazoan signal recognition particle RNA	3.48
ENSSSSCG00000029839	Metazoa_SRP	Metazoan signal recognition particle RNA	3.47
ENSSSSCG00000029605	Metazoa_SRP	Metazoan signal recognition particle RNA	3.06
ENSSSSCG00000012594	IL13RA2	Interleukin 13 receptor subunit α2	-3.09
ENSSSSCG00000029023	ARL5B	ADP-ribosylation factor-like 5B	-5.43
ENSSSSCG00000008595	APOB	Apolipoprotein B	-3.73
ENSSSSCG00000002387	GPATCH2L	G patch domain containing 2-like	-3.59
ENSSSSCG00000030247	EPM2AIP1	EPM2A (laforin) interacting protein 1	-3.57
ENSSSSCG00000024674	ABL2	v-abl Abelson murine leukemia viral oncogene homolog$_2$	-3.48
ENSSSSCG00000030726	CH242-150C11.4	CH242-150C11.4	-3.46
ENSSSSCG00000005466	ROD1	PTBP3-polypyrimidine tract binding protein 3	-3.23
ENSSSSCG00000016510	UBN2	Ubinuclein 2	-3.19
ENSSSSCG00000008909	CLOCK	Clock homolog (mouse)	-3.17
ENSSSSCG00000004616	ONECUT1	One cut homeobox 1	-3.12
ENSSSSCG00000015284	MDM4	Mdm4 p53 binding protein homolog (mouse)	-3.10
ENSSSSCG00000008292	TET3	Tet methylcytosine dioxygenase 3	-3.09
ENSSSSCG00000016119	RAPH1	Ras association (RalGDS/AF-6) and pleckstrin homology domains 1	-3.09
ENSSSSCG00000004106	LATS1	LATS, large tumor suppressor, homolog 1 (Drosophila)	-3.08
ENSSSSCG00000010604	SH3PXD2A	SH3 and PX domains 2A	-3.07
ENSSSSCG00000025182	ELK4	ELK4, ETS-domain protein (SRF accessory protein 1)	-3.04
ENSSSSCG00000002755	NFAT5	Nuclear factor of activated T-cells 5, tonicity-responsive	-3.03
ENSSSSCG00000016031	CRLR	Calcitonin receptor-like	-3.02
ENSSSSCG00000005285	GNAQ	Guanine nucleotide binding protein (G protein), q polypeptide	-3.02

Only values of log$_2$FC higher than ±3 with more than four normalized edgeR counts were taken into account. Log$_2$FC, log$_2$ fold change.

Availability of data and materials

Preprocessed RNA sequencing datasets generated during the present study are available from the corresponding author on reasonable request.

Authors' contributions

MB, JC, MP and PP designed the study. MP, PV, PZ and VP performed the experiments with animals. MB and JC performed molecular biology experiments. MB, JO, VB and PP analysed the data. MB, JO, VB and PP wrote the text.

Ethics approval and consent to participate

Approval from the Bioethical Committee from the Center for Cardiovascular Research and Development, American Heart of Poland S.A. (Ustroń, Poland) was obtained.

Consent for publication

Not applicable.

Competing interests

The authors declare that they have no competing interests.

References

1. Michalopoulos GK and DeFrances MC: Liver regeneration. Science 276: 60-66, 1997.

2. Zimmermann A: Regulation of liver regeneration. Nephrol Dial Transplant 19 (Suppl 4): iv6-iv10, 2004.

3. Palmes D and Spiegel HU: Animal models of liver regeneration. Biomaterials 25: 1601-1611, 2004.

4. Bendixen E, Danielsen M, Larsen K and Bendixen C: Advances in porcine genomics and proteomics-a toolbox for developing the pig as a model organism for molecular biomedical research. Brief Funct Genomics 9: 208-219, 2010.

5. Budai A, Fulop A, Hahn O, Onody P, Kovacs T, Nemeth T, Dunay M and Szijarto A: Animal models for associating liver partition and portal vein ligation for staged hepatectomy (ALPPS): Achievements and future perspectives. Eur Surg Res 58: 140-157, 2017.

6. Gimble JM, Katz AJ and Bunnell BA: Adipose-derived stem cells for regenerative medicine. Circ Res 100: 1249-1260, 2007.

7. Mizuno H, Tobita M and Uysal AC: Concise review: Adipose-derived stem cells as a novel tool for future regenerative medicine. Stem Cells 30: 804-810, 2012.

8. Pak J, Lee JH, Kartolo WA and Lee SH: Cartilage regeneration in human with adipose tissue-derived stem cells: Current status in clinical implications. Biomed Res Int 2016: 4702674, 2016.

9. Premaratne GU, Ma LP, Fujita M, Lin X, Bollano E and Fu M: Stromal vascular fraction transplantation as an alternative therapy for ischemic heart failure: Anti-inflammatory role. J Cardiothorac Surg 6: 43, 2011.

10. Koh YJ, Koh BI, Kim H, Joo HJ, Jin HK, Jeon J, Choi C, Lee DH, Chung JH, Cho CH, *et al*: Stromal vascular fraction from adipose tissue forms profound vascular network through the dynamic reassembly of blood endothelial cells. Arterioscler Thromb Vasc Biol 31: 1141-1150, 2011.

11. Schnitzbauer A, Lang SA, Fichtner-Feigl S, *et al*: In situ split with portal vein ligation induces rapid left lateral lobe hypertrophy enabling two-staged extended right hepatic resection. Berl Oral Presentation 35, 2010.

12. Schnitzbauer AA, Lang SA, Goessmann H, Nadalin S, Baumgart J, Farkas SA, Fichtner-Feigl S, Lorf T, Goralcyk A, Hörbelt R, *et al*: Right portal vein ligation combined with in situ splitting induces rapid left lateral liver lobe hypertrophy enabling 2-staged extended right hepatic resection in small-for-size settings. Ann Surg 255: 405-414, 2012.

13. Schadde E, Raptis DA, Schnitzbauer AA, Ardiles V, Tschuor C, Lesurtel M, Abdalla EK, Hernandez-Alejandro R, Jovine E, Machado M, *et al*: Prediction of mortality after ALPPS stage-1: An analysis of 320 patients from the international ALPPS registry. Ann Surg 262: 780-786, 2015.

14. Saidi RF, Rajeshkumar B, Shariftabrizi A, Bogdanov AA, Zheng S, Dresser K and Walter O: Human adipose-derived mesenchymal stem cells attenuate liver ischemia-reperfusion injury and promote liver regeneration. Surgery 156: 1225-1231, 2014.

15. Pascual-Miguelañez I, Salinas-Gomez J, Fernandez-Luengas D, Villar-Zarra K, Clemente LV, Garcia-Arranz M and Olmo DG: Systemic treatment of acute liver failure with adipose derived stem cells. J Invest Surg 28: 120-126, 2015.

16. Lin K, Matsubara Y, Masuda Y, Togashi K, Ohno T, Tamura T, Toyoshima Y, Sugimachi K, Toyoda M, Marc H and Douglas A: Characterization of adipose tissue-derived cells isolated with the Celution system. Cytotherapy 10: 417-426, 2008.

17. Andrews S: FastQC: A quality control tool for high throughput sequence data. Anim Sci, 2010. (http://www.bioinformatics.babraham.ac.uk/projects/fastqc/).

18. Dobin A, Davis CA, Schlesinger F, Drenkow J, Zaleski C, Jha S, Batut P, Chaisson M and Gingeras TR: STAR: Ultrafast universal RNA-seq aligner. Bioinformatics 29: 15-21, 2013.

19. Liao Y, Smyth GK and Shi W: featureCounts: An efficient general purpose program for assigning sequence reads to genomic features. Bioinformatics 30: 923-930, 2014.

20. Robinson MD, McCarthy DJ and Smyth GK: edgeR: A Bioconductor package for differential expression analysis of digital gene expression data. Bioinformatics 26: 139-140, 2010.

21. Von Mering C, Huynen M, Jaeggi D, Schmidt S, Bork P and Snel B: STRING: A database of predicted functional associations between proteins. Nucleic Acids Res 31: 258-261, 2003.

22. Szklarczyk D, Franceschini A, Wyder S, Forslund K, Heller D, Huerta-Cepas J, Simonovic M, Roth A, Santos A, Tsafou KP, *et al*: STRING v10: Protein-protein interaction networks, integrated over the tree of life. Nucleic Acids Res 43 (Database Issue): D447-D452, 2015.

23. Mi H, Huang X, Muruganujan A, Tang H, Mills C, Kang D and Thomas PD: PANTHER version 11: Expanded annotation data from gene ontology and Reactome pathways, and data analysis tool enhancements. Nucleic Acids Res 45: D183-D189, 2017.

24. Kanehisa M and Goto S: KEGG: Kyoto encyclopedia of genes and genomes. Nucleic Acids Res 28: 27-30, 2000.
25. Kanehisa M, Goto S, Sato Y, Furumichi M and Tanabe M: KEGG for integration and interpretation of large-scale molecular data sets. Nucleic Acids Res 40 (Database Issue): D109-D114, 2012.
26. Hahn E, Wick G, Pencev D and Timpl R: Distribution of basement membrane proteins in normal and fibrotic human liver: Collagen type IV, laminin, and fibronectin. Gut 21: 63-71, 1980.
27. Pöschl E, Schlötzer-Schrehardt U, Brachvogel B, Saito K, Ninomiya Y and Mayer U: Collagen IV is essential for basement membrane stability but dispensable for initiation of its assembly during early development. Development 131: 1619-1628, 2004.
28. Gressner OA, Rizk MS, Kovalenko E, Weiskirchen R and Gressner AM: Changing the pathogenetic roadmap of liver fibrosis? Where did it start; where will it go? J Gastroenterol Hepatol 23: 1024-1035, 2008.
29. Rychtrmoc D, Hubálková L, Víšková A, Libra A, Bunček M and Červinková Z: Transcriptome temporal and functional analysis of liver regeneration termination. Physiol Res 61 (Suppl 2): S77-S92, 2012.
30. Okano J, Shiota G, Matsumoto K, Yasui S, Kurimasa A, Hisatome I, Steinberg P and Murawaki Y: Hepatocyte growth factor exerts a proliferative effect on oval cells through the PI3K/AKT signaling pathway. Biochem Biophys Res Commun 309: 298-304, 2003.
31. Jackson LN, Larson SD, Silva SR, Rychahou PG, Chen LA, Qiu S, Rajaraman S and Evers BM: PI3K/Akt activation is critical for early hepatic regeneration after partial hepatectomy. Am J Physiol Gastrointest Liver Physiol 294: G1401-G1410, 2008.
32. Reiner R, Ben-Asouli Y, Krilovetzky I and Jarrous N: A role for the catalytic ribonucleoprotein RNase P in RNA polymerase III transcription. Genes Dev 20: 1621-1635, 2006.
33. Veidal SS, Karsdal MA, Vassiliadis E, Nawrocki A, Larsen MR, Nguyen QH, Hägglund P, Luo Y, Zheng Q, Vainer B and Leeming DJ: MMP mediated degradation of type VI collagen is highly associated with liver fibrosis-identification and validation of a novel biochemical marker assay. PLoS One 6: e24753, 2011.
34. Cheng W, Xiao L, Ainiwaer A, Wang Y, Wu G, Mao R, Yang Y and Bao Y: Molecular responses of radiation-induced liver damage in rats. Mol Med Rep 11: 2592-2600, 2015.
35. Zhang Y, Zhang H, Zhao Z, Lv M, Jia J, Zhang L, Tian X, Chen Y, Li B, Liu M, et al: Enhanced expression of glucose-regulated protein 78 correlates with malondialdehyde levels during the formation of liver cirrhosis in rats. Exp Ther Med 10: 2119-2125, 2015.
36. Chuang HM, Su HL, Li C, Lin SZ, Yen SY, Huang MH, Ho LI, Chiou TW and Harn HJ: The role of butylidenephthalide in targeting the microenvironment which contributes to liver fibrosis amelioration. Front Pharmacol 7: 112, 2016.
37. Kongphat W, Pudgerd A and Sridurongrit S: Hepatocyte-specific expression of constitutively active Alk5 exacerbates thioacetamide-induced liver injury in mice. Heliyon 3: e00305, 2017.
38. Ross MA, Sander CM, Kleeb TB, Watkins SC and Stolz DB: Spatiotemporal expression of angiogenesis growth factor receptors during the revascularization of regenerating rat liver. Hepatology 34: 1135-1148, 2001.
39. Koncina E, Roth L, Gonthier B and Bagnard D: Role of semaphorins during axon growth and guidance. Adv Exp Med Biol 621: 50-64, 2007.
40. Fu L, Kitamura T, Iwabuchi K, Ichinose S, Yanagida M, Ogawa H, Watanabe S, Maruyama T, Suyama M and Takamori K: Interplay of neuropilin-1 and semaphorin 3A after partial hepatectomy in rats. World J Gastroenterol 18: 5034-5041, 2012.
41. Yamamoto H, Murawaki Y and Kawasaki H: Hepatic collagen synthesis and degradation during liver regeneration after partial hepatectomy. Hepatology 21: 155-161, 1995.
42. Shimamura T, Fujisawa T, Husain SR, Kioi M, Nakajima A and Puri RK: Novel role of IL-13 in fibrosis induced by nonalcoholic steatohepatitis and its amelioration by IL-13R-directed cytotoxin in a rat model. J Immunol 181: 4656-4665, 2008.
43. Mederacke I, Hsu CC, Troeger JS, Huebener P, Mu X, Dapito DH, Pradere JP and Schwabe RF: Fate tracing reveals hepatic stellate cells as dominant contributors to liver fibrosis independent of its aetiology. Nat Commun 4: 2823, 2013.
44. Maria AT, Toupet K, Maumus M, Fonteneau G, Le Quellec A, Jorgensen C, Guilpain P and Noël D: Human adipose mesenchymal stem cells as potent anti-fibrosis therapy for systemic sclerosis. J Autoimmun 70: 31-39, 2016.
45. Tan Y, Yoshida Y, Hughes DE and Costa RH: Increased expression of hepatocyte nuclear factor 6 stimulates hepatocyte proliferation during mouse liver regeneration. Gastroenterology 130: 1283-1300, 2006.
46. Diaz B, Shani G, Pass I, Anderson D, Quintavalle M and Courtneidge SA: Tks5-dependent, nox-mediated generation of reactive oxygen species is necessary for invadopodia formation. Sci Signal 2: ra53, 2009.
47. Arvaniti E, Moulos P, Vakrakou A, Chatziantoniou C, Chadjichristos C, Kavvadas P, Charonis A and Politis PK: Whole-transcriptome analysis of UUO mouse model of renal fibrosis reveals new molecular players in kidney diseases. Sci Rep 6: 26235, 2016.